Article

Wafer-Scale Uniform Carbon Nanotube Transistors for Ultrasensitive and Label-Free Detection of Disease Biomarkers

Yuqi Liang, Mengmeng Xiao, Ding Wu, Yanxia Lin, Lijun Liu, Jianping He, Guo-Jun Zhang, Lian-Mao Peng, and Zhiyong Zhang

ACS Nano, **Just Accepted Manuscript** • DOI: 10.1021/acsnano.0c03523 • Publication Date (Web): 23 Jun 2020

Wafer-Scale Uniform Carbon Nanotube Transistors for Ultrasensitive and Label-Free Detection of Disease Biomarkers

Yuqi Liang,[1+] Mengmeng Xiao,[2+] Ding Wu,[3] Yanxia Lin,[2] Lijun Liu,[2] Jianping He,[1] Guojun Zhang,[3] Lian-Mao Peng,[1,2] Zhiyong Zhang[1,2]*

[1] Hunan Institute of Advanced Sensing and Information Technology, Xiangtan University, Hunan 411105, China

[2] Key Laboratory for the Physics and Chemistry of Nanodevices and Center for Carbon-based Electronics, Department of Electronics, Peking University, Beijing 100871, China

[3] School of Laboratory Medicine, Hubei University of Chinese Medicine, Huangjia Lake West Road, Wuhan 430065, People's Republic of China

ABSTRACT: Carbon nanotube (CNT) field-effect transistor (FET)-based biosensors have shown great potential for ultrasensitive biomarker detection but challenges remain which include unsatisfactory sensitivity, difficulty in stable functionalization, incompatibility with scalable fabrication, and un-uniformed performance. Here, we describe ultrasensitive, label-free and stable FET biosensors built on polymer-sorted high-purity semiconducting CNT films with wafer-scale fabrication and high uniformity. With a floating gate (FG) structure using an ultra-thin Y_2O_3 high κ dielectric layer, the CNT FET biosensors show amplified response and improved sensitivity compared with those sensors without Y_2O_3, which is attributed to the chemical gate-coupling effect dominates the sensor response. The CNT FG-FETs are modified to selectively detect specific disease

biomarkers, namely, DNA sequences and microvesicles (MVs), with theoretical record detection limits as low as 60 aM and 6 particles/mL, respectively. Furthermore, the biosensors exhibit highly uniform performance over the 4-inch wafer as well as superior bias stress stability. The FG CNT FET biosensors could be extended as a universal biosensor platform for the ultrasensitive detection of multiple biological molecules and applied in highly integrated and multiplexed all CNT-FET based sensor architectures.

KEYWORDS: biosensor, carbon nanotubes, field-effect transistors, DNA, extracellular microvesicles

Detecting disease biomarkers at ultralow concentrations is essential for early-stage medical diagnostics. Current methods such as quantitative real-time PCR[1] (qRT-PCR, for genetic screening) and ELISA[2] (for antibody-antigen protein systems) require the labeling of target biomolecules and involve complicated equipment, impeding their application in point-of-care (POC) devices and immediate diagnosis. Biosensor platforms such as field-effect transistor (FET) based biosensors have been considered to fulfill the next-generation medical diagnostic requirements of miniaturization, high-throughput, ultrasensitive and cost-effective alternatives to conventional methods.[3-6]

The appearance of nanomaterials and the rapid growth of semiconductor device fabrication techniques have inspired a large amount of research interests in constructing highly sensitive and integrated FET-based biosensors for next-generation medical applications.[7,8] Among the variety of nanomaterials, semiconducting carbon nanotubes (CNTs) have atomic-thickness bodies, excellent electrical properties, good biocompatibility, and good size compatibility[9-12] and thus have been considered ideal channel materials to construct ultrasensitive FET biosensors. Although significant

advances have been achieved by using either individual CNTs or CNT network films to fabricate FET biosensors.[13,14] the fabrication of reproductive, stable and ultrasensitive CNT FET-based biosensors on a large scale is still challenging. First, lacking in reproducible semiconducting CNT materials and high-throughput device fabrication[15-20] in wafer scale inhibit the practical application of CNT FET biosensors. In recent years, great progresses have been made on the preparation of polymer-sorted highly pure semiconducting CNT solutions films which has promoted the wafer-scale fabrication of CNT FETs.[21-25] However, their application in high performance biosensors is still in their infancy. Secondly, none of the reported CNT FET biosensors were designed with optimized structures. In traditional CNT FET biosensors, channels were directly linked to the biomolecules and exposed to the test solution, which is a complex environment;[15,26,27] thus, various interaction mechanisms modulate the channel conduction simultaneously. The multiple competing mechanisms will have complex effects on the channel conduction and may lower the sensitivity of the biosensor.[28] This issue not only prevents CNT networks from acting as reproducible sensor elements, but confused people with the inconsistent current response and low sensitivity with the charged biomolecules.[15,16,29,30] Furthermore, the common modification methods utilizing in CNT biosensors with Au nanoparticles,[15] defects[31] or π-π stacking functional molecules[32] as linkers to connect probe bio-functional molecules to the CNT channel will damage the initial properties of CNTs or be invalid for functionalization on polymer-sorted semiconducting CNTs, which are the most mature CNT materials for next generation electronics.[23,25,33]

In this article, we will explore reproducible and ultrasensitive CNT FET biosensors through combining device structure optimization and material advancement to overcome previous limitations. We revisit the mechanism of conventional CNT FET biosensors and develop a floating gate(FG)

CNT FET biosensor with 6 nm Y_2O_3 insulating layer to avoid the complex interactions in the former cases.[34,35] We note that although the dielectric layer increases the distance between biomolecules and CNT channel, it provides a versatile platform for functionalization and effectively improves the sensor response and reproducibility, which is attributed to the chemical gate-coupling effect dominates the sensor response with the series of the dielectric layer capacitance. As demonstrations, FG CNT FETs are used to construct biosensors for detecting specific DNA sequences for Patau syndrome screening and MVs secreted by hepatoma carcinoma cells with theoretical record detection limits as low as 60 aM and 6 particles/mL, respectively. Furthermore, the biosensors exhibit highly uniform performance over the 4-inch wafer as well as superior bias stress stability. The recent advances of CNT based integrated circuits together with the biosensor platform we developed here indicates the great potential in highly integrated and multiplexed all CNT-FET based sensor architectures.[22-25,33]

RESULTS AND DISCUSSION

Wafer-Scaled Sensor Devices Fabrication and Characterization. Polymer-sorted solution-derived CNTs with semiconducting purity higher than 99.9% were deposited on a 4-inch Si/SiO_2 wafer (Supporting Information, S1) to form a randomly oriented film with high uniformity (Figure S1).[24] A process based on photolithography (Supporting Information, S2; Figure S2) was used to fabricate CNT FET biosensors on a 4-inch wafer, and the device arrays are shown in Figure 1a. Here we use an ultrathin Y_2O_3 film of 6 nm (equivalent oxide thickness (EOT) of 2.3 nm)[35] to cover the whole CNT channel and then assembled Au nanoparticles on Y_2O_3 as linkers to connect biological probes; And Y_2O_3 film-passivated CNT FETs (Figure 1b) are shown to act as floating gate

(FG) FET biosensors. All fabrication steps are wafer-scale and compatible with mainstream complementary metal-oxide-semiconductor (CMOS) manufacturing technologies, which will help to promote practical applications of biosensors. The photograph of Figure 1c shows a biosensor chip containing 22 FETs, in which contacts and leads (to measurement pads) are passivated by a photoresist layer to prevent current leakage, side electrochemistry reaction and work-function modulation of the metal contacts and leads in ion liquid, and a window in the channel is exposed (Figure 1d-e). The exposed channel region was decorated with Au nanoparticles, which are uniformly distributed on Y_2O_3 (Figure 1f， Figure S3) and act as efficient linkers to connect biological probes. [36-38]

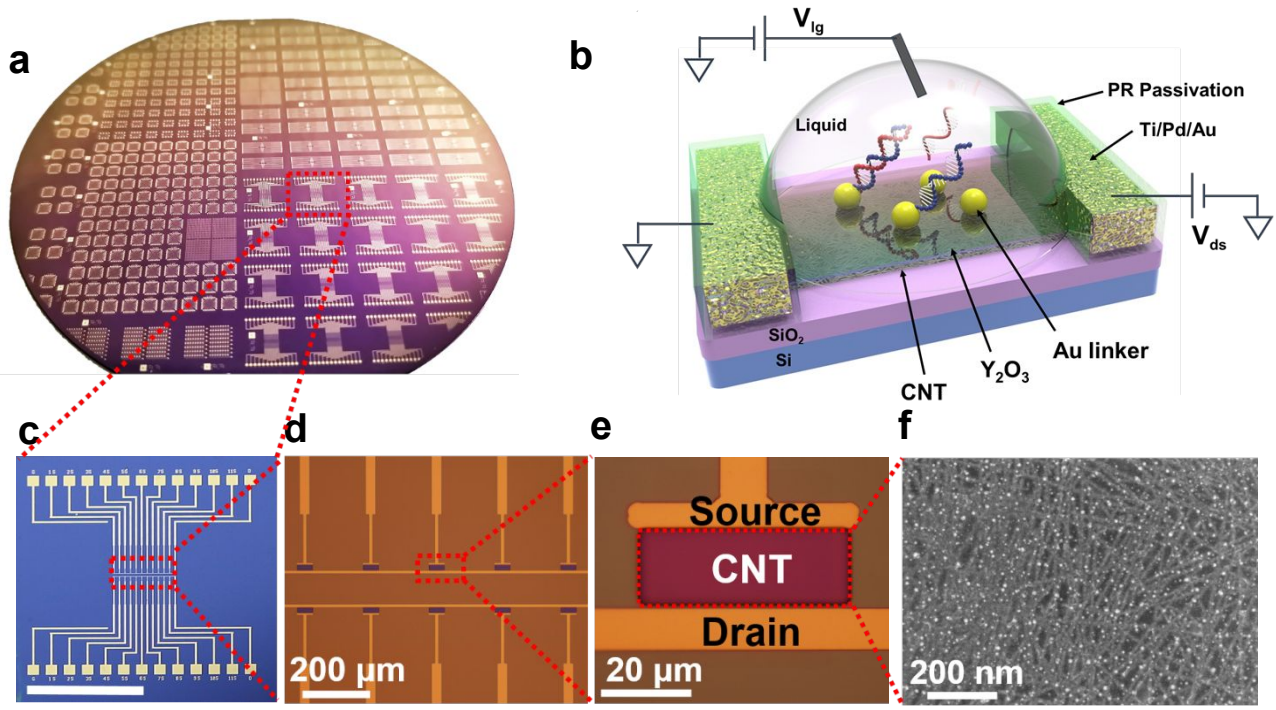

Figure 1. The wafer-scale fabrication of CNT FG-FETs for biosensor arrays. (a) Photograph image of the fabricated CNT device array on a 4-inch wafer. One die for the biosensor array is outlined in red. (b) Schematic diagram of a CNT FG-FET biosensor. (c) Optical micrograph of a die for a biosensor array. The scale bar is 5 mm. (d) A further magnified optical micrograph showing the

core channel regions of the biosensor array, (e) The optical micrograph of one FET biosensor. The meatal contact and lead were passivated by photoresist. (f) Scanning electron microscopy (SEM) image showing a part of the channel of the device in Au NPs were uniformly distributed on the Y_2O_3/CNT film.

For utility as a biosensor platform, FETs should be fabricated with high yield, reliability and performance uniformity, and it is important to statistically characterize wafer-scale CNT FETs. Ninety randomly selected CNT FETs with liquid solution gates (Supporting Information, S3; Figure S4) exhibited highly uniform transfer characteristics with low variation (Figure 2a). All transistors presented *p*-type FET characteristics with current on/off ratios as high as 10^5, demonstrating 100% yield and the ultrahigh semiconducting purity of our sorted CNTs. In particular, the hysteresis-free and low subthreshold slope (SS) of 68 mV/dec (Figure 2b) indicated that CNT FETs can provide stable and maximized conduction change to the charge change on the FG, which is vital to the desired reliable detection. The linear output curves at low bias (Figure 2c) benefit from ohmic contacts. The statistical performance distributions in Figure 2d and e and supporting information (Figure S5) confirm the uniformity of CNT FETs: SS ranges from 60 to 90 mV/dec with an average value of 76 mV/dec (Figure 2d), and V_{th} obeys the normal distribution with an expectation of -0.17 V and a small standard deviation of 17 mV (Figure 2e). The FET biosensor generally works in either a linear regime for quantitative analysis or in a subthreshold regime for much higher sensitivity,[39] while V_{th} and SS are key parameters in the two regimes. Therefore, the excellent uniformity of SS and V_{th} in a 4-inch wafer will ensure reliable detection for bio-molecules (Supporting Information, S4) through the FET biosensor in each mode. In addition, the statistical distributions of the device

performance after FG fabricated are also presented in Figure S6, indicating a great successive uniformity. Bias stress measurements (Figure 2f; Figure S7a) indicate that the device presents long-term (at least 1000 s here) stability for sensing applications. Highly uniform CNT FETs with high performance and stability over a 4-inch wafer provide a solid device platform for the development of sensitive and reliable biosensors.

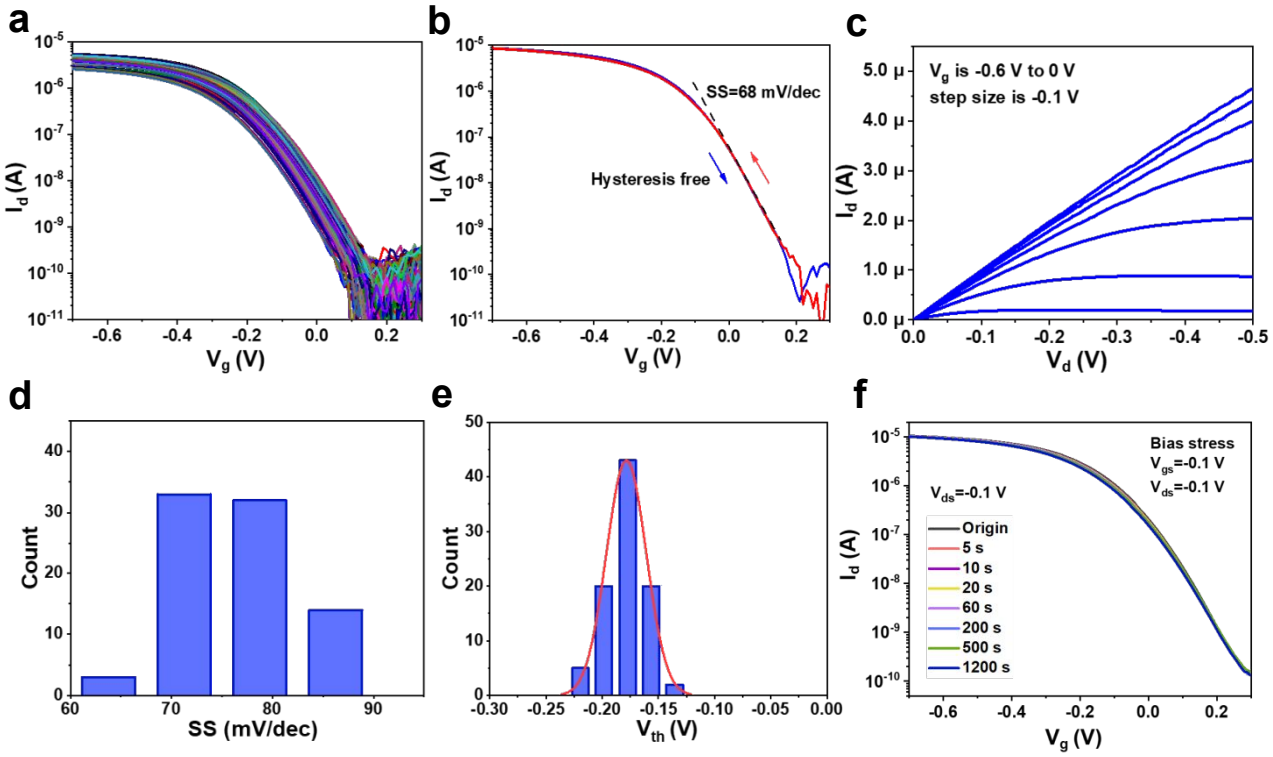

Figure 2. Electrical characteristics of wafer-scale fabricated CNT FETs by using liquid gates. (a) Transfer curves of 90 FETs at V_{ds}= -0.1 V. (b) Transfer characteristics of a typical CNT FET by sweeping V_{gs} with different directions. (c) Output properties of a typical CNT FET. (d,e) Statistical distributions of SS and V_{th} in the 90 FETs in Figure 2a. (f) The transfer characteristics of a typical CNT FET after different times of continuous bias stress. The FET is continuously biased with V_{gs}=V_{ds}= -0.1 V before every transfer curve measurement.

Ultrasensitive Detection of Small Molecules-DNA. The first kind of biosensor is designed according to the process flow in Figure 3a to detect a specific DNA sequence (Table S1, part of chromosome 13, typical biomarker for Patau syndrome, which causes serious physical and mental abnormalities).[40,41] Au nanoparticles (Au NPs) are decorated on the Y_2O_3 layer of CNT FG-FETs and act as linkers to capture the sulfhydrylation probe molecules by Au-S covalent bonds (Figure 1b,3a). The CNT/Y_2O_3/Au NPs stacked layer forms the FG-FET sensing platform. To selectively detect specific DNA fragments (here, chromosome 13), the probe DNA sequences described in Table S1 are immobilized by the Au NPs, and then the DNA biosensor is ready.

Figure 3b illuminates how the consecutive modification steps affect the performance of the CNT FETs. After growing the Y_2O_3 film on the CNT film channel, the on-state drain-source current (I_{ds}) and transconductance (g_m) decrease since the total gate capacitance drastically declines owing to the introduction of the additional Y_2O_3 film capacitance in series with the electric double layer (EDL) capacitance. Conduction of the FETs further decreased slightly after Au NPs decoration, mainly owing to the reduction in EDL capacitance and surface potential fluctuation induced by Au NPs (Supporting Information S5, Figure S8). It should be mentioned that no obvious change in SS and no shift of the transfer curves was observed after the introduction of Y_2O_3 or Au NPs, indicating that there was no significant doping to the channel nor interface states introduced by both the Y_2O_3 and Au NPs modification. However, with the immobilization of probe DNA, CNT FETs exhibit a 30 mV V_{th} shift in the I_d-V_g curve with invisible changes in g_m and SS, indicating *p*-type electrostatic doping induced by the negative charge gating of the probe DNAs.[28]

We measured the response of the as-prepared CNT FET biosensors to the chromosome 13 target DNA (Table S1) with concentrations ranging from 100 aM to 1 fM (Figure 3c). The hybridizations

take place in high concentration of 1 × phosphate buffer solution (PBS) to reduce the range of electrostatic repulsion between probe and target DNA and all the electrical measurement were performed in 0.1 × PBS to increase the Debye length to 2.4 nm which is in the same range of the 30-base DNA sequence length.[41] The transfer curve shifted positively with increasing target DNA concentration since the negative charges on the gate introduced by the hybridized target DNA increased with the target concentration. The response of a biosensor is generally defined as $Response=(I_{ds}-I_{ds0})/I_{ds0}$ at certain V_{ds} and $V_{ds,}$ where I_{ds0} and I_{ds} are the drain current before and after target DNA hybridization. We calculated the sensor response in the liner working regime of the CNT FG-FET with V_{ds}= -0.1 V and V_{gs} = -0.7 V. The sensor response to target DNA of different concentration is summarized in Figure 3e, in which the inset represents the static responses of five biosensors at different concentrations. The response increased with increasing concentration of the target DNA with an almost linear relation with the logarithmic concentration(Supporting Information S4), and reaches up to the maximum response (162%) at a 1 fM concentration which was among the highest responses in FET-based biosensors.[15,27] The FG sensors shows a record theoretical LOD of 60 aM (based on the cross point of extrapolated line with the blank control group) for DNA hybridization in aqueous environment, which corresponds to around 360 copies in our 10μL sample droplet. This LOD is much higher than the detectable sensitivity of fM ~ pM level in the fluorescence microscope used in PCR[1] and make it possible to use the technique in a clinical setting without PCR amplification or labeling steps. Selectivity tests (Figure 3d) indicate that the response to complementary DNA is significantly higher than that to mismatched DNA (Table S1), and then the biosensor exhibits excellent selectivity to the target DNA. The weak response of biosensors to mismatched DNAs is mainly attributed to nonspecific physical adsorption of the DNAs and does

not affect the excellent specificity of our biosensors.

Real-time detection measurements (Figure 3f) were performed to check the sensitivity, reliability and selectivity of the CNT FG-FET biosensors. When buffer solution was injected, the drain current increased substantially and then immediately returned to the baseline, which means that the injection perturbance was transient and restorable. The added solution of mismatched DNA (m-DNA) induced little but notable change to the drain current, indicating that nonspecific binding was successfully suppressed. Then, solutions with increasing target DNA concentrations are added to the biosensor in turn. The introduction of target DNA led to a distinct current increment in 50 s, and the change amplitude increased with increasing concentration, which was consistent with the trend in static detection. This demonstrates that FG-FET sensors are able to monitor target DNA molecules at a concentration of 100 aM in a very short time, which may have great potential in the rapid diagnosis field.

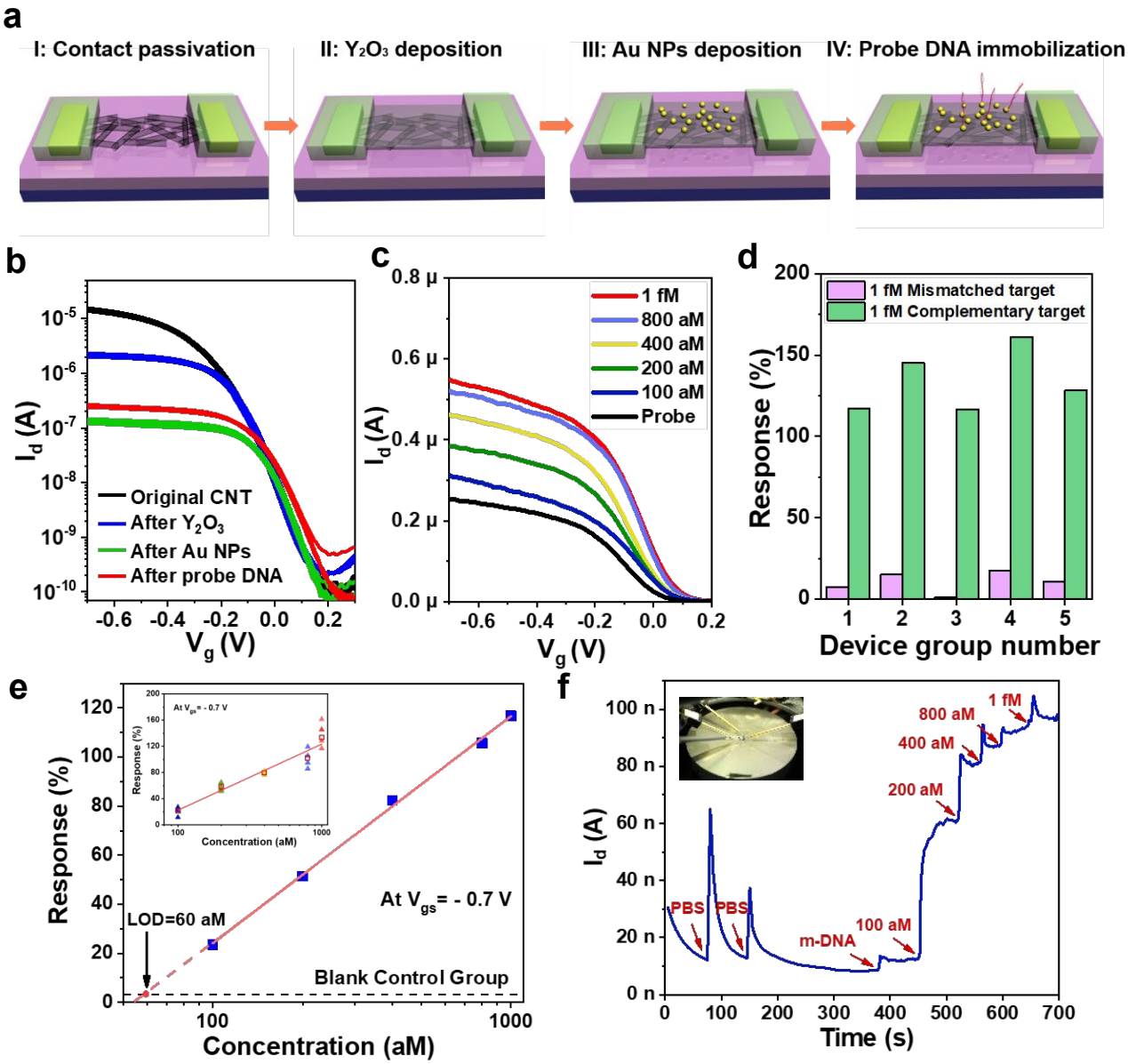

Figure 3. Fabrication and characteristics of the CNT FG-FET biosensor platforms for DNA detection. (a) The fabrication process of FG-FET biosensors based on CNT FETs. (b) Transfer curve evolution of the five CNT FETs during the decorating process to obtain biosensors: pristine (black), deposition of Y_2O_3 (blue) and Au NPs (green), and immobilization of the probe DNA (red). All measurements were carried out in 0.1 × PBS electrolyte. V_{ds}= -0.1 V (c) Transfer curve evolution of the CNT FG-FET biosensor recorded after the introduction of various target concentrations ranging from 100 aM to 1 fM. (d) The response of five groups of sensor devices to mismatched and

complementary DNA at the same concentration. (e) The calibration curve of DNA detection corresponding to Figure 3c at V_{gs}= -0.7 V and V_{ds}= -0.1 V. The black dash line represents a blank control group submerged in 0.1 × PBS solution. The extension of liner fitting curves gives the theoretical LOD of 60 aM. Inset: the response-concentration relationship of five different biosensors. Average responses of five devices is liner fitted with the logarithmic value of DNA concertation. (f) Real-time recording of the response of a biosensor to different additions, including PBS, mismatched DNA and target DNA, at different concentrations. The drain current was monitored in 0.1 × PBS with $V_{gs} = V_{ds}$= -0.1 V during the test.

Sensing Mechanism of FG CNT FET. Ultrasensitive and reliable detection mainly originates from the adoption of an FG-FET structure in which the conduction channel is isolated from solution by an ultrathin insulator. Figure 4 illuminates the difference between FG-FET biosensors and normal FET biosensors. With the channel un-passivated and directly exposed to the solution, the conductance of normal FET biosensor is affected by coupled interaction with CNT channel, including electrostatic gating, changes in gate coupling, Au/probe-induced scattering to carrier, and Schottky barrier effects.[28] The competing mechanisms will affect the channel conduction simultaneously and lower the response in channel current (or sensitivity of the biosensor). For example, biomolecule immobilization and hybridization will cause a local carrier scattering effect around the Au islands and chemical gating effect in the CNT channel competitively, and two mechanisms lead to opposite changes in conduction if the immobilized target DNA is negatively charged.[28,29] In FG-FETs, the channel was isolated from the solution by Y_2O_3 passivation layer. The interaction only take place on the FG with the dominate mechanism for detection of target-induced

electrostatic gating effect (Figure 4a,c). Y_2O_3 was chosen as the gate dielectric for its excellent interface with carbon nanotube and high κ value.[23] What should be mentioned is that, the increased distance by Y_2O_3 layer will not reduce the absorption electrostatic control over the channel as the ultra-thin body of the CNT and the highly efficient gate with ultrathin Y_2O_3 and large EDL capacitance. As We further performed experiments to compare the sensing characteristics of the two kinds of biosensors (Figure 4e,f). When detecting ultralow concentration target DNAs (Figure 4e), FG-FET biosensors exhibit distinct and uniform positive responses, whereas normal FET biosensors suffer from small and uncertain responses. When detecting high-concentration target DNAs (Figure 4f), normal FET biosensors exhibit a negative response (current decrease) since the scattering effect dominates the conduction of the CNT channel. The negative response to negatively charged targets is always observed in reported CNT FET biosensors.[15,19,42] The FG-FET biosensors still exhibit an increased positive response, and the response is much higher than that of normal FET biosensors. The results clarified the confusing results in previous reports that most of the response of negatively charged biomolecules induced a conductance decreasing response.

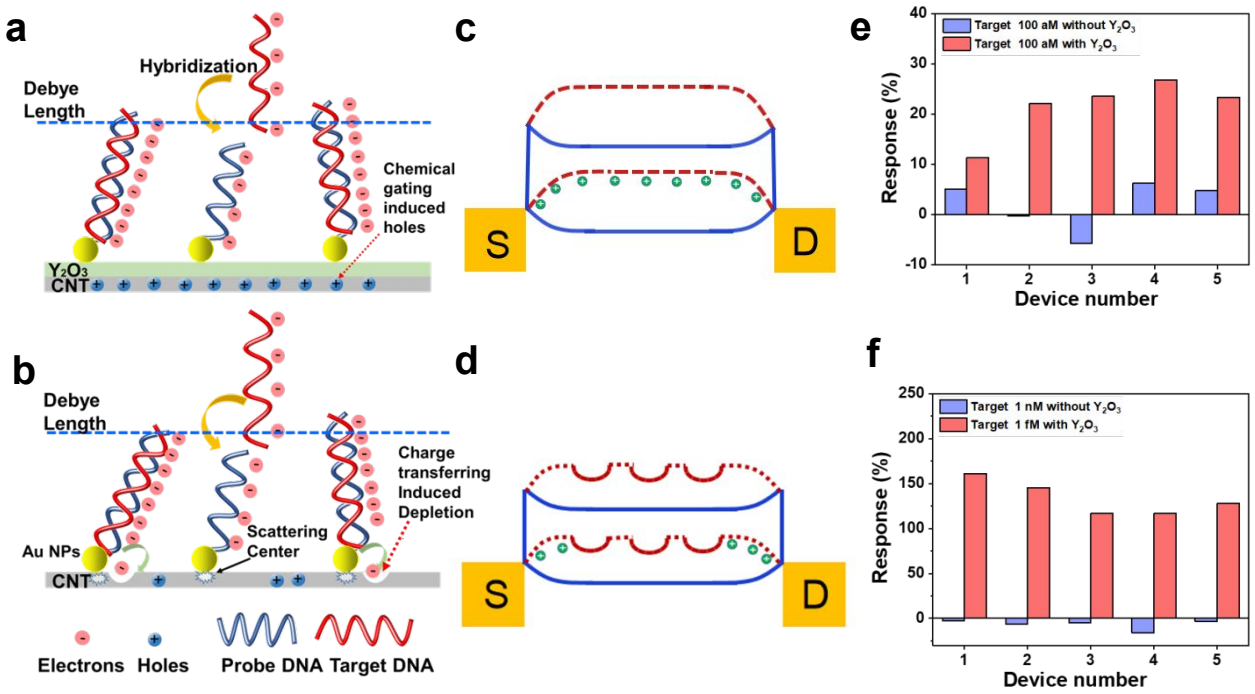

Figure 4. Sensing mechanism analysis for the CNT FET biosensor. (a) Schematic representation of the sensing mechanism in an FG-FET biosensor. The short black line next DNA indicating the DNA molecules is negative charged in PBS at a PH of 7.4. The probe DNA (blue DNAs) immobilized on the Au nanoparticles (yellow particles) surface, with a random direction due to its structure flexibility and most of the length beneath the Debye length boundary (blue dash line). The DNA hybridization will mainly lead to the chemical gating induced holes in the channel. (b) Schematic representation of the sensing mechanism in a normal FET biosensor. The direct modification of Au nanoparticles and charge transfer after the DNA hybridization will introduce the scattering effect and charge transferring induced depletion areas in the channel. (c) Energy band diagrams for the FG-FETs before (blue solid lines) and after (red dash lines) biomolecule hybridization. (d) Energy band diagrams for normal FETs before (blue solid lines) and after (red dash lines) biomolecule hybridization. (e,f) Comparison of the responses of FG-FETs and normal FETs to low (Figure 4e) and high (Figure 4f) concentrations of target biomolecules.

Quantitative Detection of MVs Derived From Cancer Cells. We now consider to demonstrate the application of the CNT FG-FET biosensor for the quantitative detection of MVs derived from human liver cancer cells (HepG2). Microvesicles are lipid bilayer-enclosed membrane vesicles packaged with the molecular signature (including membrane surface and intracellular proteins, nucleic acids) of their parental cells.[43] Tumor-derived MVs have been explored as a promising biomarker because of their high concentration (up to 6×10^6 particles/μL) and stability in the blood circulation.[44,45] However, current molecular analyses of MVs generally require large numbers of MVs to be concentrated and processed using time-consuming western blotting or ELISA,[46] making them impractical in a typical clinical setting.

Our biosensors were formed by functionalizing Au NPs with the sulfhydrylation aptamer sequence TLS11 (Table S2), which can specifically bind to the membrane surface protein of HepG2 MVs.[47,48] MVs were cultured from HepG2 cell lines (Supporting Information, S6; Figure S10) and isolated by a sequence of centrifugation steps[48,49] as depicted in Figure 5a. Detection measurements showed that the response increased with the concentration of MV solution, as shown in Figure S11 and Figure 5b. The aptamer-modified FG-FET biosensors show the wide-range detection of MVs from 6 particles/μL to 6×10^6 particles/μL, with an theoretical LOD of 6×10^{-3} particles/μL. The main interaction to enable the detection of MVs by aptamer-modified FETs is that the target incorporation will induce conformational changes in probes (TLS11) decorated on Y_2O_3.[50] The conformation change of probes has two effects on the channel conduction of the FET. On the one hand, negatively charged aptamer phosphodiester backbones in the transformed TLS11 molecules become nearer to the semiconductor channel, which leads to a change in the effective charges on the gate and induces

the V_{th} positive drift of the biosensors. On the other hand, the transformation of probes results in position changes in EDL/Au NPs/Y_2O_3 and then changes the effective gate capacitance of FETs, leading to an increase in the transconductance (Figure S11). The two mechanisms both lead to conduction increases, and then the FET biosensors exhibited high sensitivity for MV detection.

The selectivity of the biosensors for the detection of HepG2 MVs was investigated through comparing sensing responses to AFP (alpha-fetoprotein, 70 μg/mL), CEA (carcinoembryonic antigen, 4.5 μg/mL) and HL-7702-derived MVs (the MVs of normal liver cells, 6×10^2 particles/μL) and 0.1 × PBS (the control blank group), as shown in Figure 5c. The response to MVs (40%) was much higher than that to other control groups (lower than 12%), indicating excellent selectivity of the aptamer-modified FET biosensor for HepG2 MVs.

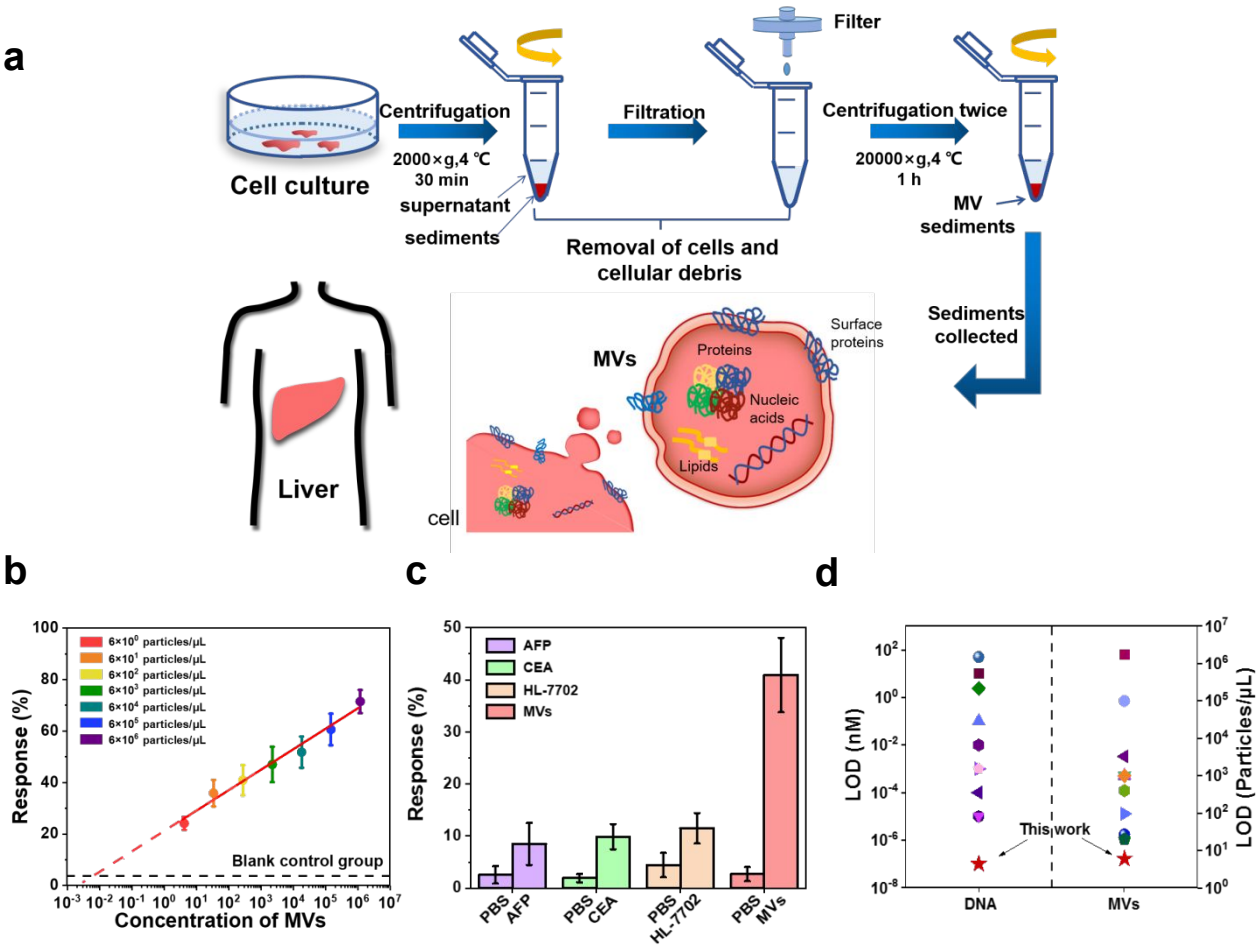

Figure 5. Detection of MVs by the CNT FG-FET biosensor platform. (a) Isolation procedure of MVs derived from HepG2 cells. (b) The calibration curve of aptamer-modified CNT FG-FET biosensors detecting the MVs at different concentrations (6 particles/μL ~ 6 × 10^6 particles/μL). V_{ds}= -0.1 V and V_{gs} = -0.7 V. The black dashed line represents the noise level (~3.7) from the blank control test in 1 × PBS solution**.** (c) Response comparison between HepG2-MVs and other control cancer markers, including AFP (70 μg/mL), CEA (4.2 μg/mL) and the normal hepatocyte MV HL-7702 at the same concentration of 6 × 10^2 particles/μL). The error bars show the standard deviation. (d) Benchmarking (by LOD) our biosensor platform with previously reported biosensors for DNA and MV detection. (Reference data see Table S3, Table S4 in Supporting Information)

Benchmarking of the Sensor Performance. We benchmarked our CNT FG-FET biosensors by LOD in comparison with other technologies, including both optical and electrochemical biosensors based on graphene and 2D materials (see Table S3,4), as shown in Figure 5d. For fair comparison, the LOD was chosen as the lowest of concertation we detected in experiment. The CNT FG-FET biosensors exhibited much lower LODs than other nanomaterial-based FET biosensors for the detection of DNAs or MVs (Figure 5d), which means the highest sensitivity in nanomaterial-based FET biosensors. With the ability to detect a few hundreds of DNA molecules or a couple of MVs in the sample solution, our results show the possibility to detect small molecules and the large cell-structures on the same sensor platform by multi-functionalization on the FG and raise hopes for the low cost and rapid detection of individual molecules and cell structures in real serum. The ultrahigh sensitivity accompanied by wafer-scale fabrication, excellent uniformity and reliability originate from the co-optimization of CNT materials, device structure and fabrication process and most likely promote the practical application of CNT FG-FET biosensors. In addition, CNT FG-FETs can be easily reformed to biosensors for the detection of other biological molecules through decorating suitable probes on Au NPs, which is there, maybe a common platform to construct various biosensors. In very recent years, great progress has been achieved on CNT-based CMOS integrated circuits (ICs),[22,23,35] and on-chip integration of biosensor arrays and signal processing schemes will become feasible owing to the compatibility of FG-FET biosensors and CMOS FETs built on CNT films.

CONCLUSIONS

In this article, we have demonstrated the label-free FG-FET biosensors built on high purity

semiconducting CNT film as highly sensitive, large scale uniform and reliable bio-sensing platforms using CMOS compatible process. The FG structure by inserting an ultra-thin high κ dielectric layer of Y_2O_3 film between Au linkers and CNT channel enables the decouple of ambiguous interactions with the channel to an univocal interaction with the FG, contributing to amplify the sensor response and enhance the sensors' sensitivity and reliability. The CNT FG-FET biosensor platforms were modified to selectively and quantitatively detect the specific DNA sequences and MVs, with the extrapolated LOD of 60 aM and 6 particles/mL separately, which set the record sensitivity of FET type biosensors for DNA and MVs detections. The CNT FG-FETs can be extended as a universal biosensor platform to perform ultrasensitive detection for special biological molecules through functioning the corresponding probes on Au nanoparticles, and even realize multi-function detections of a variety of biological molecules on the same chip. The CNT FG-FET biosensor has the similar architecture and process flow with high performance logic CNT devices, laying a foundation for the mass production of biosensors for multi-biomarkers detection and integrated with the CNT based ICs processors on the same chip in the future.

EXPERIMENTAL METHODS

Functionalization of Probe DNA Sequences with CNT FG-FET Biosensors. The DNA sequence with 5' modification with sulfhydryl for Patau syndrome screening was provided by the National Research Institute for Family Planning of China. All of the DNA sequences were custom-synthesized by Sangon Biotech (Shanghai, China). The probe DNA sediments were diluted to 100 μM with 1 × PBS and activated with tris (2-carboxyethyl) phosphine hydrochloride (TCEP, from Sigma-Aldrich) for 1 h at room temperature. The probe DNAs are covalently linked to the Au NPs in the channel by

immersing the FET in the probe DNA solutions for 12 h. These FETs are then washed with 1 × PBS and deionized water repeatedly to remove the excess probe DNAs, which are nonspecifically adsorbed in the channel. Subsequently, 2 mM 6-mercapto-1-hexanol (MCH, from J&K Scientific) was added to the channel of the FG-FET for 1 h to deactivate and block the excess reactive groups remaining on the Au surface. Finally, the FETs are immersed in 0.1 × PBS buffer again for 30 min and then can be used for the following sensing experiments. The aptamer DNA sequences of TLS11 were used as probes to detect HepG2 MVs based on previous reports. The modification process is similar to the probe DNA used above.

Biosensor Performance Characteristics. There are two common modes to characterize the sensor performance. For the static test, the target DNAs or MVs used in the experiment were diluted with 1 × PBS to serial dilution. The modified biosensors are immersed in 1 × PBS buffer solution containing target molecules for approximately 2 h to ensure complete hybridization. These biosensors are subsequently washed by a method similar to the previous rinse process. The transfer characteristics of the biosensors were measured in 0.1 × PBS before and after target hybridization. In the real-time test, 0.1 × PBS is added to the test chamber as the basic test environment. The target DNA solutions were diluted with 0.1 × PBS. The addition volume each time is controlled at 2 μL to eliminate the volume change influence.

ASSOCIATED CONTENT

Supporting Information

The Supporting Information is available free of charge *via* the Internet at http://pubs.acs.org.

Additional data including the preparation of CNTs network film, AFM and SEM characterization, device fabrication process and schematic, the liquid gated CNT FETs and FG-FET biosensors measurement method and additional electrical performance, the influence of device performance on the sensor response, the isolation process and characterization of MVs, the sequences of DNA and aptamer used in this work and benchmarking references.

AUTHOR INFORMATION

Corresponding Author

*E-mail: (Z. Y. Z.)zyzhang@pku.edu.cn

Author Contributions

Z.Z. and M.X. supervised and designed the project. Y. L and M.X. fabricated the devices and performed the sensing experiments. D.W. and G.Z. performed the isolation and characterization experiments of MVs. M.X., Y.L. and Z.Z. analyzed the experimental data and co-wrote the manuscript. All of the authors discussed the results and commented on the manuscript.

[+]These authors contributed equally to this work.

ACKNOWLEDGMENTS

This work was supported by the National Key Research & Development Program (Grant No. 2016YFA0201901), the National Natural Science Foundation of China (Grant No. 61888102) and China Postdoctoral Science Foundation funded project (Grant No.2019M660325).

REFERENCES

(1) Bustin, S. A.; Mueller, R. Real-Time Reverse Transcription PCR (qRT-PCR) and Its Potential Use in Clinical Diagnosis. *Clin. Sci.* **2005**, *109*, 365-379.

(2) Lequin, R. M. Enzyme Immunoassay (EIA)/Enzyme-Linked Immunosorbent Assay (ELISA). *Clin. Chem.* **2005**, *51*, 2415-2418.

(3) Cui, Y.; Wei, Q. Q.; Park, H. K.; Lieber, C. M. Nanowire Nanosensors for Highly Sensitive and Selective Detection of Biological and Chemical Species. *Science* **2001**, *293*, 1289-1292.

(4) Zheng, G.; Patolsky, F.; Cui, Y.; Wang, W. U.; Lieber, C. M. Multiplexed Electrical Detection of Cancer Markers with Nanowire Sensor Arrays. *Nat. Biotechnol.* **2005**, *23*, 1294-1301.

(5) Seichepine, F.; Rothe, J.; Dudina, A.; Hierlemann, A.; Frey, U. Dielectrophoresis-Assisted Integration of 1024 Carbon Nanotube Sensors into a CMOS Microsystem. *Adv. Mater.* **2017**, *29*, 1606852.

(6) Zhang, A. Q.; Lieber, C. M. Nano-Bioelectronics. *Chem. Rev.* **2016**, *116*, 215-257.

(7) Naylor, C. H.; Kybert, N. J.; Schneier, C.; Xi, J.; Romero, G.; Saven, J. G.; Liu, R. Y.; Johnson, A. T. C. Scalable Production of Molybdenum Disulfide Based Biosensors. *ACS Nano* **2016**, *10*, 6173-6179.

(8) Xu, G. Y.; Abbott, J.; Qin, L.; Yeung, K. Y. M.; Song, Y.; Yoon, H.; Kong, J.; Ham, D. Electrophoretic and Field-Effect Graphene for All-Electrical DNA Array Technology. *Nat. Commun.* **2014**, *5*, 4866.

(9) Kong, J.; Franklin, N. R.; Zhou, C. W.; Chapline, M. G.; Peng, S.; Cho, K. J.; Dai, H. J. Nanotube Molecular Wires as Chemical Sensors. *Science* **2000**, *287*, 622-625.

(10) Chen, R. J.; Bangsaruntip, S.; Drouvalakis, K. A.; Kam, N. W. S.; Shim, M.; Li, Y. M.; Kim, W.; Utz, P. J.; Dai, H. J. Noncovalent Functionalization of Carbon Nanotubes for Highly Specific

Electronic Biosensors. *Proc. Natl. Acad. Sci. U. S. A.* **2003**, *100*, 4984-4989.

(11) Balasubramanian, K.; Kern, K. 25th Anniversary Article: Label-Free Electrical Biodetection Using Carbon Nanostructures. *Adv. Mater.* **2014**, *26*, 1154-1175.

(12) Munzer, A. M.; Michael, Z. R.; Star, A. Carbon Nanotubes for the Label-Free Detection of Biomarkers. *ACS Nano* **2013**, *7*, 7448-7453.

(13) Hu, P. A.; Zhang, J.; Li, L.; Wang, Z. L.; O'Neill, W.; Estrela, P. Carbon Nanostructure-Based Field-Effect Transistors for Label-Free Chemical/Biological Sensors. *Sensors* **2010**, *10*, 5133-5159.

(14) Menard-Moyon, C.; Kostarelos, K.; Prato, M.; Bianco, A. Functionalized Carbon Nanotubes for Probing and Modulating Molecular Functions. *Chem. Biol.* **2010**, *17*, 107-115.

(15) Ko, J. W.; Woo, J. M.; Ahn, J.; Cheon, J. H.; Lim, J. H.; Kim, S. H.; Chun, H.; Kim, E.; Park, Y. J. Multi-Order Dynamic Range DNA Sensor Using a Gold Decorated SWCNT Random Network. *ACS Nano* **2011**, *5*, 4365-4372.

(16) Maehashi, K.; Katsura, T.; Kerman, K.; Takamura, Y.; Matsumoto, K.; Tamiya, E. Label-Free Protein Biosensor Based on Aptamer-Modified Carbon Nanotube Field-Effect Transistors. *Anal. Chem.* **2007**, *79*, 782-787.

(17) So, H.-M.; Won, K.; Kim, Y. H.; Kim, B.-K.; Ryu, B. H.; Na, P. S.; Kim, H.; Lee, J.-O. Single-Walled Carbon Nanotube Biosensors Using Aptamers as Molecular Recognition Elements. *J. Am. Chem. Soc.* **2005**, *127*, 11906-11907.

(18) Sorgenfrei, S.; Chiu, C. Y.; Gonzalez, R. L.; Yu, Y. J.; Kim, P.; Nuckolls, C.; Shepard, K. L. Label-Free Single-Molecule Detection of DNA-Hybridization Kinetics with a Carbon Nanotube Field-Effect Transistor. *Nat. Nanotechnol.* **2011**, *6*, 125-131.

(19) Zheng, H. Y.; Alsager, O. A.; Wood, C. S.; Hodgkiss, J. M.; Plank, N. O. V. Carbon Nanotube Field Effect Transistor Aptasensors for Estrogen Detection in Liquids. *J. Vac. Sci. Technol. B* **2015**, *33*, 06F904.

(20) Hills, G.; Lau, C.; Wright, A.; Fuller, S.; Bishop, M. D.; Srimani, T.; Kanhaiya, P.; Ho, R.; Amer, A.; Stein, Y.; Murphy, D.; Arvind; Chandrakasan, A.; Shulaker, M. M. Modern Microprocessor Built from Complementary Carbon Nanotube Transistors. Nature 2019, 572, 595-602.

(21) Gu, J. T.; Han, J.; Liu, D.; Yu, X. Q.; Kang, L. X.; Qiu, S.; Jin, H. H.; Li, H. B.; Li, Q. W.; Zhang, J. Solution-Processable High-Purity Semiconducting SWCNTs for Large-Area Fabrication of High-Performance Thin-Film Transistors. *Small* **2016**, *12*, 4993-4999.

(22) Yang, Y. J.; Ding, L.; Han, J.; Zhang, Z. Y.; Peng, L. M. High-Performance Complementary Transistors and Medium-Scale Integrated Circuits Based on Carbon Nanotube Thin Films. *ACS Nano* **2017**, *11*, 4124-4132.

(23) Chen, B. Y.; Zhang, P. P.; Ding, L.; Han, J.; Qiu, S.; Li, Q. W.; Zhang, Z. Y.; Peng, L. M. Highly Uniform Carbon Nanotube Field-Effect Transistors and Medium Scale Integrated Circuits. *Nano Lett.* **2016**, *16*, 5120-5128.

(24) Xiao, M. M.; Liang, S. B.; Han, J.; Zhong, D. L.; Liu, J. X.; Zhang, Z. Y.; Peng, L. M. Batch Fabrication of Ultrasensitive Carbon Nanotube Hydrogen Sensors with Sub-ppm Detection Limit. *ACS Sens.* **2018**, *3*, 749-756.

(25) Peng, L. M.; Zhang, Z. Y.; Qiu, C. G. Carbon Nanotube Digital Electronics. *Nat. Electron.* **2019**, *2*, 499-505.

(26) Gui, E. L.; Li, L.-J.; Zhang, K.; Xu, Y.; Dong, X.; Ho, X.; Lee, P. S.; Kasim, J.; Shen, Z. X.;

Rogers, J. A.; Mhaisalkar, S. G. DNA Sensing by Field-Effect Transistors Based on Networks of Carbon Nanotubes. *J. Am. Chem. Soc.* **2007**, *129*, 14427-14432.

(27) Dong, X.; Lau, C. M.; Lohani, A.; Mhaisalkar, S. G.; Kasim, J.; Shen, Z.; Ho, X.; Rogers, J. A.; Li, L.-J. Electrical Detection of Femtomolar DNA *via* Gold-Nanoparticle Enhancement in Carbon-Nanotube-Network Field-Effect Transistors. *Adv. Mater.* **2008**, *20*, 2389-2393.

(28) Heller, I.; Janssens, A. M.; Mannik, J.; Minot, E. D.; Lemay, S. G.; Dekker, C. Identifying the Mechanism of Biosensing with Carbon Nanotube Transistors. *Nano Lett.* **2008**, *8*, 591-595.

(29) Pacios, M.; Martin-Fernandez, I.; Borrise, X.; del Valle, M.; Bartroli, J.; Lora-Tamayo, E.; Godignon, P.; Perez-Murano, F.; Esplandiu, M. J. Real Time Protein Recognition in a Liquid-Gated Carbon Nanotube Field-Effect Transistor Modified with Aptamers. *Nanoscale* **2012**, *4*, 5917-5923.

(30) Okuda, S.; Okamoto, S.; Ohno, Y.; Maehashi, K.; Inoue, K.; Matsumoto, K. Horizontally Aligned Carbon Nanotubes on a Quartz Substrate for Chemical and Biological Sensing. *J. Phys. Chem. C* **2012**, *116*, 19490-19495.

(31) Banerjee, S.; Hemraj-Benny, T.; Wong, S. S. Covalent Surface Chemistry of Single-Walled Carbon Nanotubes. *Adv. Mater.* **2005**, *17*, 17-29.

(32) Calvaresi, M.; Zerbetto, F. The Devil and Holy Water: Protein and Carbon Nanotube Hybrids. *Acc. Chem. Res.* **2013**, *46*, 2454-2463.

(33) Hills, G.; Lau, C.; Wright, A.; Fuller, S.; Bishop, M. D.; Srimani, T.; Kanhaiya, P.; Ho, R.; Amer, A.; Stein, Y.; Murphy, D.; Arvind; Chandrakasan, A.;Shulaker, M. M. Modern Microprocessor Built from Complementary Carbon Nanotube Transistors. *Nature* **2019**, *572*, 595-602.

(34) Ding, L.; Zhang, Z.; Su, J.; Li, Q.;Peng, L. M. Exploration of Yttria Films as Gate Dielectrics

in Sub-50 nm Carbon Nanotube Field-Effect Transistors. *Nanoscale* **2014**, *6*, 11316-11321.

(35) Liang, S. B.; Zhang, Z. Y.; Si, J.; Zhong, D. L.;Peng, L. M. High-Performance Carbon-Nanotube-Based Complementary Field-Effect-Transistors and Integrated Circuits with Yttrium Oxide. *Appl. Phys. Lett.* **2014**, *105*, 063101.

(36) Negandary, M. Aptamers in Nanostructure-Based Electrochemical Biosensors for Cardiac Biomarkers and Cancer Biomarkers: A review. *Biosens. Bioelectron.* **2020**, *152*, 112018.

(37) Hakkinen H. The Gold-Sulfur Interface at The Nanoscale. *Nat. Chem.* **2012**, *4*, 443-455.

(38) Grandbois, M.; Beyer, M.; Rief, M.; Clausen-Schaumann, H.; Gaub, H. E. How Strong Is a Covalent Bond? *Science* **1999**, *283*, 1727-1730.

(39) Sarkar, D.; Liu, W.; Xie, X.; Anselmo, A. C.; Mitragotri, S.; Banerjee, K. MoS_2 Field-Effect Transistor for Next-Generation Label-Free Biosensors. *ACS Nano* **2014**, *8*, 3992-4003.

(40) Patau's Syndrome. NHS Website. https://www.nhs.uk/conditions/pataus-syndrome (accessed on 20 February, 2020).

(41) Liu, J. X.; Chen, X. H.; Wang, Q. Q.; Xiao, M. M.; Zhong, D. L.; Sun, W.; Zhang, G. Y.; Zhang, Z. Y. Ultrasensitive Monolayer MoS_2 Field-Effect Transistor Based DNA Sensors for Screening of Down Syndrome. *Nano Lett.* **2019**, *19*, 1437-1444.

(42) Kurkina, T.; Vlandas, A.; Ahmad, A.; Kern, K.; Balasubramanian, K. Label-Free Detection of Few Copies of DNA with Carbon Nanotube Impedance Biosensors. *Angew. Chem., Int. Ed.* **2011**, *50*, 3710-3714.

(43) Tkach, M.; Thery, C. Communication by Extracellular Vesicles: Where We Are and Where We Need to Go. *Cell* **2016**, *164*, 1226-1232.

(44) Thery, C.; Ostrowski, M.; Segura, E. Membrane Vesicles as Conveyors of Immune

Responses. *Nat. Rev. Immunol.* **2009**, *9*, 581-593.

(45) Colombo, M.; Raposo, G.; Thery, C. Biogenesis, Secretion, and Intercellular Interactions of Exosomes and Other Extracellular Vesicles. *Annu. Rev. Cell Dev. Biol.* **2014**, *30*, 255-289.

(46) Witwer, K. W.; Buzas, E. I.; Bemis, L. T.; Bora, A.; Lasser, C.; Lotvall, J.; Nolte-'t Hoen, E. N.; Piper, M. G.; Sivaraman, S.; Skog, J.; Thery, C.; Wauben, M. H.; Hochberg, F. Standardization of Sample Collection, Isolation and Analysis Methods in Extracellular Vesicle Research. *J. Extracell. Vesicles* **2013**, 2, 20360.

(47) Kashefi-Kheyrabadi, L.; Mehrgardi, M. A.; Wiechec, E.; Turner, A. P. F.; Tiwari, A. Ultrasensitive Detection of Human Liver Hepatocellular Carcinoma Cells Using a Label-Free Aptasensor. *Anal. Chem.* **2014**, *86*, 4956-4960.

(48) Wu, D.; Yu, Y.; Jin, D.; Xiao, M. M.; Zhang, Z. Y.;Zhang, G. J., Dual-Aptamer Modified Graphene Field-Effect Transistor Nanosensor for Label-Free and Specific Detection of Hepatocellular Carcinoma-Derived Microvesicles. *Anal. Chem.* **2020**, *92*, 4006-4015.

(49) Wu, D.; Zhang, H.; Jin, D.; Yu, Y.; Pang, D. W.; Xiao, M. M.; Zhang, Z. L.; Zhang, Z. Y.; Zhang, G. J. Microvesicle Detection by a Reduced Graphene Oxide Field-Effect Transistor Biosensor Based on a Membrane Biotinylation Strategy. *Analyst* **2019**, *144*, 6055-6063.

(50) Nakatsuka, N.; Yang, K. A.; Abendroth, J. M.; Cheung, K. M.; Xu, X. B.; Yang, H. Y.; Zhao, C. Z.; Zhu, B. W.; Rim, Y. S.; Yang, Y.; Weiss, P. S.; Stojanovic, M. N.; Andrews, A. M. Aptamer-Field-Effect Transistors Overcome Debye Length Limitations for Small-Molecule Sensing. *Science* **2018**, *362*, 319-324.

For Table of Contents Only